Osteoarthritis and Cartilage 22 (2014) 1007–1017

Osteoarthritis and Cartilage

Endoplasmic reticulum stress-induced apoptosis contributes to articular cartilage degeneration *via* C/EBP homologous protein

Y. Uehara †, J. Hirose ‡*, S. Yamabe †, N. Okamoto †, T. Okada †, S. Oyadomari §, H. Mizuta †

† *Department of Orthopaedic Surgery, Faculty of Life Sciences, Kumamoto University, 1-1-1 Honjo, Chuo-ku, Kumamoto 860-8556, Japan*
‡ *Department of Orthopaedic Surgery, Kumamoto University Hospital, 1-1-1 Honjo, Chuo-ku, Kumamoto 860-8556, Japan*
§ *Division of Molecular Biology, Institute for Genome Research, The University of Tokushima, 3-18-15 Kuramoto, Tokushima 770-8503, Japan*

ARTICLE INFO

Article history:
Received 30 September 2013
Accepted 23 April 2014

Keywords:
Endoplasmic reticulum stress
C/EBP homologous protein
Chondrocyte apoptosis
Cartilage degeneration

SUMMARY

Objective: When endoplasmic reticulum (ER) stress, i.e., the excessive accumulation of unfolded proteins in ER, endangers homeostasis, apoptosis is induced by C/EBP homologous protein (Chop). In osteoarthritis (OA) cartilage, Chop expression and apoptosis increase as degeneration progresses. We investigated the role of Chop in murine chondrocyte apoptosis and in the progression of cartilage degeneration.
Method: We induced experimental OA in *Chop*-knockout ($Chop^{-/-}$) mice by medial collateral ligament transection and meniscectomy and compared cartilage degeneration, apoptosis, and ER stress in $Chop^{-/-}$- and wild-type ($Chop^{+/+}$) mice. In our *in vitro* experiments we treated murine $Chop^{-/-}$ chondrocytes with the ER stress inducer tunicamycin (TM) and evaluated apoptosis, ER stress, and chondrocyte function.
Results: In vivo, the degree of ER stress was similar in $Chop^{-/-}$- and $Chop^{+/+}$ mice. However, in $Chop^{-/-}$ mice apoptosis and cartilage degeneration were lower by 26.4% and 42.4% at 4 weeks, by 26.8% and 44.9% at 8 weeks, and by 26.9% and 32.3% at 12 weeks after surgery than $Chop^{+/+}$ mice, respectively. *In vitro*, the degree of ER stress induction by TM was similar in $Chop^{-/-}$- and $Chop^{+/+}$ chondrocytes. On the other hand, apoptosis was 55.3% lower and the suppression of *collagen type II* and *aggrecan* mRNA was 21.0% and 23.3% less, and the increase of *matrix metalloproteinase-13* mRNA was 20.0% less in $Chop^{-/-}$- than $Chop^{+/+}$ chondrocytes.
Conclusion: Our results indicate that Chop plays a direct role in chondrocyte apoptosis and that Chop-mediated apoptosis contributes to the progression of cartilage degeneration in mice.

Introduction

Chondrocytes, the only cells in articular cartilage, maintain cartilage homeostasis by regulating the synthesis and enzymatic breakdown of the extracellular matrix (ECM)[1,2]. Loss of homeostasis due to chondrocyte apoptosis leads to the destruction of articular cartilage characteristic of osteoarthritis (OA)[2]. As cartilage degeneration progresses with the degree of chondrocyte apoptosis[3,4], it is considered to play an important role in the onset and progression of OA[5,6]. Apoptosis is triggered when death stimuli activate one of three distinct cell death pathways; the plasma membrane death receptor-, the mitochondrial-, or the endoplasmic reticulum (ER) stress pathway[7].

ER stress, defined as a disequilibrium between the load of unfolded proteins in the ER and the capacity of the organelle, leads to the accumulation of unfolded or misfolded proteins[8]. After the multi-step activation of ER stress sensors (IRE1α, ATF6, and PERK) on the ER membrane, three distinct ER stress response phases (unfolded protein response, UPR) are induced to maintain ER homeostasis. Their translational attenuation reduces the load of newly synthesized proteins, induces ER chaperones such as 78 kDa glucose-regulated protein (Grp78) to enhance folding activity in the ER, and degrades unfolded or misfolded proteins *via* the ubiquitin-proteasome system in the cytosol[9]. Excessive ER stress compromises homeostasis and results in apoptosis[10]. Apoptotic events are mediated by transcriptional activation of the gene for C/EBP homologous protein (Chop)[11]. Chop directly regulates death effectors

* Address correspondence and reprint requests to: J. Hirose, Department of Orthopaedic Surgery, Kumamoto University Hospital, 1-1-1 Honjo, Chuo-ku, Kumamoto 860-8556, Japan. Tel: 81-96-373-5226; Fax: 81-96-373-5228.
E-mail addresses: ue1nen@yahoo.co.jp (Y. Uehara), hirojun-mk@umin.ac.jp, hirojunkmc@yahoo.co.jp (J. Hirose), soichiro_yamabe@yahoo.co.jp (S. Yamabe), nobuoka9999@fc.kuh.kumamoto-u.ac.jp (N. Okamoto), tatsuya-okada@fc.kuh.kumamoto-u.ac.jp (T. Okada), oyadomar@genome.tokushima-u.ac.jp (S. Oyadomari), mizuta@kumamoto-u.ac.jp (H. Mizuta).

http://dx.doi.org/10.1016/j.joca.2014.04.025
1063-4584/

such as Bcl-2 and Bim that determine cell death or survival and eventually lead to apoptosis *via* the activation of caspase-3[12–14].

Elsewhere we reported that ER stress-induced apoptosis and the expression of CHOP increased as degeneration in human OA cartilage progressed[15]. In cultured chondrocytes, the ER stress inducer tunicamycin (TM) mediates Chop expression and apoptosis, decreases *aggrecan* (*Acan*) and *collagen type II* (*Col2*) mRNA expression[16], and increases the expression of *matrix metalloproteinase-13* (*Mmp13*) mRNA[17]. We also reported[18] that ER stress-induced apoptosis mediated by nitric oxide was suppressed by *Chop* knockdown in rat chondrocytes. Using our murine OA model, we demonstrated that 4 weeks after surgery the progression of cartilage degeneration was less marked in *Chop*-knockout ($Chop^{-/-}$) mice[19], suggesting that Chop plays an important role in ER stress-induced apoptosis that results in cartilage degeneration. To elucidate the relationship between ER stress and apoptosis and cartilage degeneration we assessed the direct role of Chop in chondrocytes from $Chop^{-/-}$ mice and compared the degree of ER stress, apoptosis, and cartilage degeneration in $Chop^{-/-}$- and $Chop^{+/+}$ mice.

Methods

Animals

$Chop^{+/+}$ C57BL/6J mice were from Japan SLC (Hamamatsu, Japan), $Chop^{-/-}$ mice[20] with a C57BL/6 × C57BL/6 background were provided by the Department of Molecular Genetics, Kumamoto University. Our study was approved by the Animal Care and Use Committee of Kumamoto University.

OA model

To prepare our murine OA model[21] we exposed the right knee joint of anesthetized 8-week-old mice after medial capsular incision, transected the medial collateral ligament, and removed the medial meniscus. The left knee joint was sham-operated. The whole knee joint from $Chop^{+/+}$- and $Chop^{-/-}$ mice was harvested immediately after surgery (week 0), and at 4-, 8-, and 12 weeks later ($n = 10$ at each time point).

Preparation of histological samples

All harvested tissues were fixed in 4% paraformaldehyde (PFA; 4°C, 18 h), treated with 70% ethanol overnight (4°C) to remove fat, decalcified in 10% EDTA (4°C, 2 weeks), and embedded in paraffin. Coronal 4-μm-thick sections were cut from the center of weight-bearing areas in the medial compartment of the knee. The first section was used for Safranin-O staining; subsequent sections were used for TUNEL- and immunohistochemical staining.

Safranin-O staining

Sections were stained with Safranin-O fast-green and studied under a light microscope. The histological severity of cartilage degeneration was evaluated by the modified Mankin scoring system[22]. The recorded scores were derived from the combined scores of two observers (YU and KT) who assigned grades to the articular cartilage structure, to tidemark duplication, Safranin-O staining, and to fibrocartilage, chondrocyte clones in uncalcified cartilage, hypertrophic chondrocytes in calcified cartilage, and subchondral bone. They were blinded to the Chop status of the mice; they assigned the OA grade by consensus.

Terminal deoxynucleotidyl transferase-mediated deoxyuridine triphosphate nick-end labeling (TUNEL) staining

TUNEL staining was with the *in situ* cell death detection kit AP (Roche Diagnostics GmbH, Mannheim, Germany). TUNEL solution was added at 37°C for 1 h; counterstaining was with propidium iodide (PI; Invitrogen, Carlsbad, CA). The samples were examined in the dark using a laser scanning confocal microscope (FV300, Olympus, Tokyo, Japan). The percentage of TUNEL-positive chondrocytes was calculated from the number of total cells and the number of positive cells present from the superficial- to the deep layer in the proximal tibial cartilage[23]. The degree of DNA fragmentation was evaluated semiquantitatively by the ratio of TUNEL-positive cells.

Immunohistochemistry

The expression level of Chop, the spliced form of X-box binding protein 1 (Xbp1s), Grp78, cleaved caspase-3 (CC3), Col2, and Mmp13 in cartilage were evaluated immunohistochemically. Rabbit anti-Chop- and goat anti-Grp78 polyclonal antibody (pAb) were from Santa Cruz Biotechnology Inc. (Santa Cruz, CA). Rabbit anti-Xbp1s pAb was from BioLegend (San Diego, CA), and rabbit anti-CC3 monoclonal Ab from Cell Signaling Technology (Danvers, MA). Rabbit anti-Col2- and rabbit anti-Mmp13 pAb was from Abcam (Cambridge, UK). The secondary antibodies were visualized by using Histofine MAX-PO (R) and Histofine MAX-PO (G) (Nichirei Bioscience Inc., Tokyo, Japan) and Alexa Fluor®488 (Invitrogen). Sections were deparaffinized and rehydrated gradually. After treating the samples with proteinase K (Dako, Glostrup, Denmark) for 15 min at room temperature (RT) for antigen retrieval they were washed in phosphate buffered saline (PBS). The sections were then incubated in 0.3% hydrogen peroxide/methanol for 30 min to block endogenous peroxidase activities, and washed in PBS. Non-specific binding sites were blocked with normal goat serum (Nichirei Bioscience) prior to incubation with anti-Chop, anti-Xbp1s, anti-CC3, anti-Col2, and anti-Mmp13 antibody or with normal rabbit serum (Nichirei Bioscience) before incubation (30 min, RT) with anti-Grp78 antibody. They were then incubated with primary antibodies diluted in PBS (Chop, 1:200; Xbp1s, 1:200; Grp78, 1:300; CC3, 1:500; Col2, 1:200; Mmp13, 1:200) at 4°C for 18 h, washed in PBS, and incubated (30 min, RT) with the appropriate secondary antibodies (Alexa Fluor®488 for Chop, Histofine MAX-PO (R) for Xbp1s, CC3, Col2, and Mmp13, Histofine MAX-PO (G) for Grp78). Sections incubated with anti-Chop antibody were counterstained with PI and observed in the dark under a laser scanning confocal microscope (FV300). Staining for antibodies other than Mmp13 was with 3,3′-diaminobenzide tetrahydrochloride (DAB; Invitrogen) followed by counterstaining with hematoxylin; observation was under a light microscope. Mmp13 was counterstained with methyl green (Vector Laboratories Inc., Burlingame, CA) before detection with DAB. Sections incubated without primary antibody were the negative controls. As with TUNEL staining, each protein expression level other than Col2 was evaluated semiquantitatively by calculating the total percentage of cells positive for each protein in the section from the superficial layer to the deep layer in the proximal tibial cartilage. The Col2 expression in the cartilage was measured semiquantitatively with a staining H-score[24]. The score was multiplied by the median % staining area score for each category (none, weak, moderate, and strong) in order to derive an overall staining score between 0 and 264.

Chondrocyte culture

Knee and hip joint cartilage slices from 5-week-old male *Chop*$^{+/+}$- and *Chop*$^{-/-}$ mice were dissociated enzymatically in 0.25% trypsin/EDTA (Gibco, Gaithersburg, MD) and 0.2% collagenase (Gibco) at 37°C for 2 h. Primary chondrocytes were plated in high-density monolayers (1.0×10^5 cells/cm^2) and cultured in Dulbecco's modified Eagle's medium (DMEM) (Nacalai Tesque Inc., Kyoto, Japan) containing 10% fetal bovine serum (FBS; Gibco). All *in vitro* experiments were performed in triplicate, and the results were confirmed by at least three independent experiments.

Induction of ER stress

Media were replaced with serum-free DMEM/Ham's F-12. After 12 h, chondrocytes were incubated for 12 h with DMEM/Ham's F-12 medium containing 0.5% FBS and 1 μg/ml TM (Calbiochem, San Diego, CA) (TM$^+$) or with TM-free medium (TM$^-$).

RNA extraction and reverse transfection with mRNA

Total RNA from cultured chondrocytes was extracted with the RNeasy mini kit (Qiagen, Valencia, CA) and DNase (Qiagen). The high-capacity RNA-to-cDNA kit (Applied Biosystems, Foster, CA) was used for reverse-transcription from RNA to cDNA.

Real-time reverse transcriptase-polymerase chain reaction (RT-PCR)

Quantitative real-time RT-PCR assay was on an Applied Biosystems 7500 PCR system. TaqMan universal PCR master mix and TaqMan gene expression assays for *Chop* (Mm001135937_g1), *Grp78* (Mm00517690_g1), *Col2a1* (Mm00491889_m1), *Acan* (Mm00545807_m1), *Mmp13* (Mm01168713_m1), and *Gapdh* (Mm99999915_g1) were from Applied Biosystems. The cycling parameters were 2 min at 50°C and 10 min at 95°C; 40 cycles of 15 s at 95°C and 1 min at 60°C. The expression level of each gene was quantified using the ΔΔCt method and normalized to the internal control (*Gapdh* mRNA).

Evaluation of the splicing of Xbp1 mRNA

The splicing of *Xbp1* mRNA was evaluated by RT-PCR assay using *Xbp1* mRNA and PstI restriction enzyme[25]. PCR amplification of *Xbp1* mRNA was with TaKaRa LA Taq (Takara, Kyoto, Japan) and the GeneAmp PCR system 9700 (Applied Biosystems). The primer pair for Xbp1 was 5′-GAGCAGCAAGTGGTGGATTT-3′ (sense) and 5′-AGGGTCCAACTTGTCCAGAA-3′ (anti-sense). Denaturation was at 94°C, followed by 35 denaturation cycles at 94°C for 30 s, annealing at 56°C for 30 s, and extension at 72°C for 30 s. Both the spliced- (*Xbp1s*) and unspliced (*Xbp1u*) form of *Xbp1* mRNA in the PCR products were amplified by a primer we designed. As this 26-bp region contains a PstI restriction site, the PCR products of *Xbp1s* mRNA whose 26-bp region was excised by Ire1α were not cut by the PstI restriction enzyme. The PCR products of *Xbp1u* mRNA containing a PstI restriction site were cut. After all PCR products were incubated with the PstI restriction enzyme (37°C, 2 h) and electrophoresed on 2% agarose gels containing ethidium bromide, *Xbp1s* PCR products were visualized as 323 bp; *Xbp1u* PCR products were separated into 228- and 116 bp.

Western blotting

The chondrocytes were washed with ice-cold PBS and lysed in RIPA buffer (including 50 mM Tris/HCl (pH 7.6), 1% Nonidet P-40, 150 mM NaCl, 0.1% sodium dodecyl sulfate (SDS), 0.5% sodium deoxycholate, and protease inhibitor cocktail; Nacalai Tesque Inc.). All protein concentrations were measured with the Lowry protein assay[26]. Chondrocyte lysates (35 μg of protein/lane) dissolved in 2× sample buffer (including 50 mM Tris/HCl (pH 6.8), 20% glycerol, 4% SDS, 0.02% bromophenol blue, and 5% 2-mercaptoethanol) were heated (5 min, 95°C), separated by SDS/PAGE, and electrotransferred onto Immobilon transfer membranes (Millipore, Billerica, MA). Protein Ladder One (Nacalai Tesque Inc.) was used as a molecular marker. The membranes were blocked (30 min, RT) with 4% Block Ace (DS Pharma Biomedical, Osaka, Japan), washed three times (5 min each at RT) with Tris-buffered saline (TBS) containing Tween-20, incubated (44°C, 12 h) with mouse anti-Grp78- (Santa Cruz Biotechnology) or mouse anti-Chop monoclonal antibody (Santa Cruz Biotechnology), washed three times with TBS containing Tween-20, incubated (1 h, RT) with horseradish peroxidase-conjugated goat antibody against mouse IgG (Santa Cruz Biotechnology), and the immunoreactive proteins were detected with Chemi-Lumi One Super (Nacalai Tesque Inc.) using a luminescent image analyzer (EZ-capture2; ATTO, Tokyo, Japan).

TUNEL staining and cleaved caspase-3 immunostaining

Cultured chondrocytes were fixed with 4% PFA (4°C, 1 h), washed in PBS, and apoptotic chondrocytes were stained using the *in situ* cell death detection kit AP used for TUNEL staining in our *in vivo* evaluations. Rabbit anti-CC3 antibody (Cell Signaling Technology) and Alexa Fluor®488 goat anti-rabbit IgG (Invitrogen) as a secondary antibody were used for CC3 immunostaining. After chondrocyte nuclei were counterstained with PI, stained chondrocytes were observed in the dark under an FV300 laser scanning confocal microscope.

Enzyme-linked immunosorbent assay (ELISA)

Apoptosis of cultured chondrocytes was analyzed with cell death detection ELISA^{Plus} (Roche Diagnostics GmbH) and evaluated by the ratio of absorbance in TM$^-$ cells. In each experiment we determined the amount of protein in cell lysates in separate wells using the Quick Start Bradford protein assay (Bio-Rad Laboratories, Richmond, CA) to normalize the extent of cellular apoptosis.

Statistical analysis

All data are expressed as the mean ± 95% confidence intervals. The Student's *t*-test was used to analyze differences between *Chop*$^{+/+}$- and *Chop*$^{-/-}$ mice in the modified Mankin score, in the percentage of TUNEL-positive cells and cells immunohistochemically positive for the proteins, and in the staining H-score at week 0, 4, 8, and 12 weeks. It was also used to analyze the differences between *Chop*$^{+/+}$- and *Chop*$^{-/-}$ chondrocytes, and between TM$^-$ and TM$^+$ in *Chop*, *Grp78*, *Col2a1*, *Acan*, and *Mmp13* mRNA expression and ELISA for the detection of apoptosis. One-way analysis of variance (ANOVA) with Bonferroni *post hoc* correction was performed to analyze the differences among four time points in the modified Mankin score, in the percentage of TUNEL-positive cells and cells immunohistochemically positive for the proteins, and in the staining H-score in *Chop*$^{+/+}$- and *Chop*$^{-/-}$ mice. Differences of $P < 0.05$ were considered statistically significant. All statistical analyses were with StatView version 5.0 (SAS Institute Inc., Cary, NC).

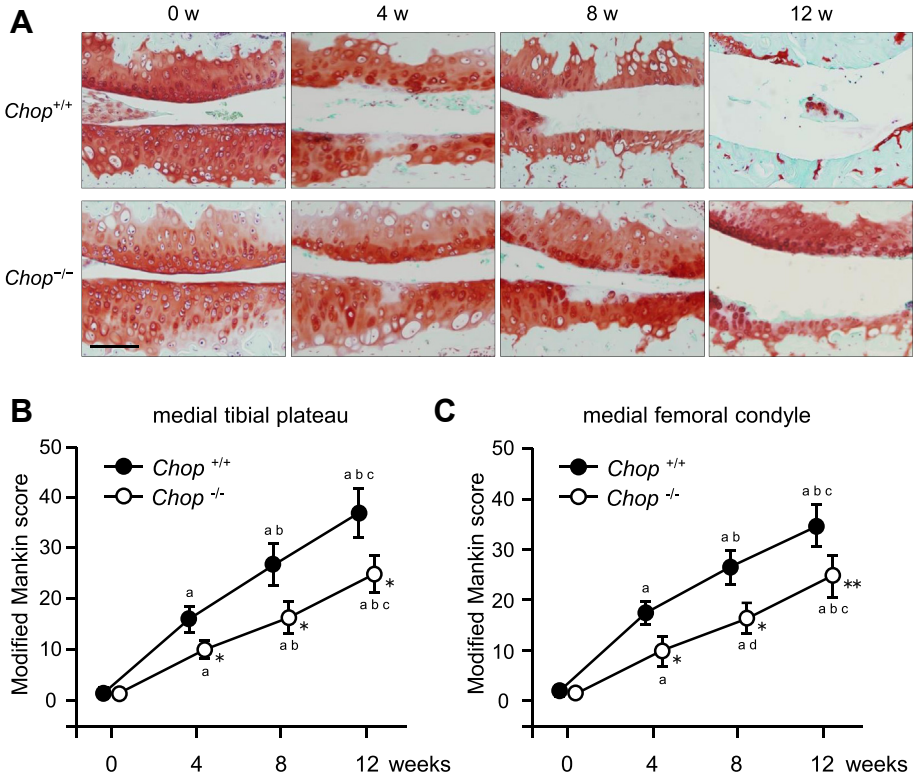

Fig. 1. Time course of cartilage degeneration in a murine model of OA. Safranin-O staining showed matrix degradation in the proximal tibial and distal femoral cartilage. The histological severity of degeneration was evaluated by the modified Mankin scoring system ($n = 10$ per experimental group and time point). (A) Gradual cartilage degeneration observed during the 12-week postoperative observation period was less severe in *Chop*$^{-/-}$- than *Chop*$^{+/+}$ mice. (B) The modified Mankin scores for tibial cartilage were significantly lower in *Chop*$^{-/-}$- than *Chop*$^{+/+}$ mice at 4, 8, and 12 weeks. (C) The modified Mankin scores for femoral cartilage were also significantly lower in *Chop*$^{-/-}$- than *Chop*$^{+/+}$ mice at 4, 8, and 12 weeks. Data are expressed as the mean (symbols) ± 95% confidence intervals (error bar). Scale bar = 100 μm, original magnification ×200. a = $P < 0.001$ vs week 0, b = $P < 0.001$ vs week 4, c = $P < 0.001$ vs week 8, d = $P = 0.002$ vs week 4 in each group of mice by ANOVA with Bonferroni *post hoc* correction. *$P < 0.001$, **$P = 0.001$ vs *Chop*$^{+/+}$ mice by the Student's *t*-test.

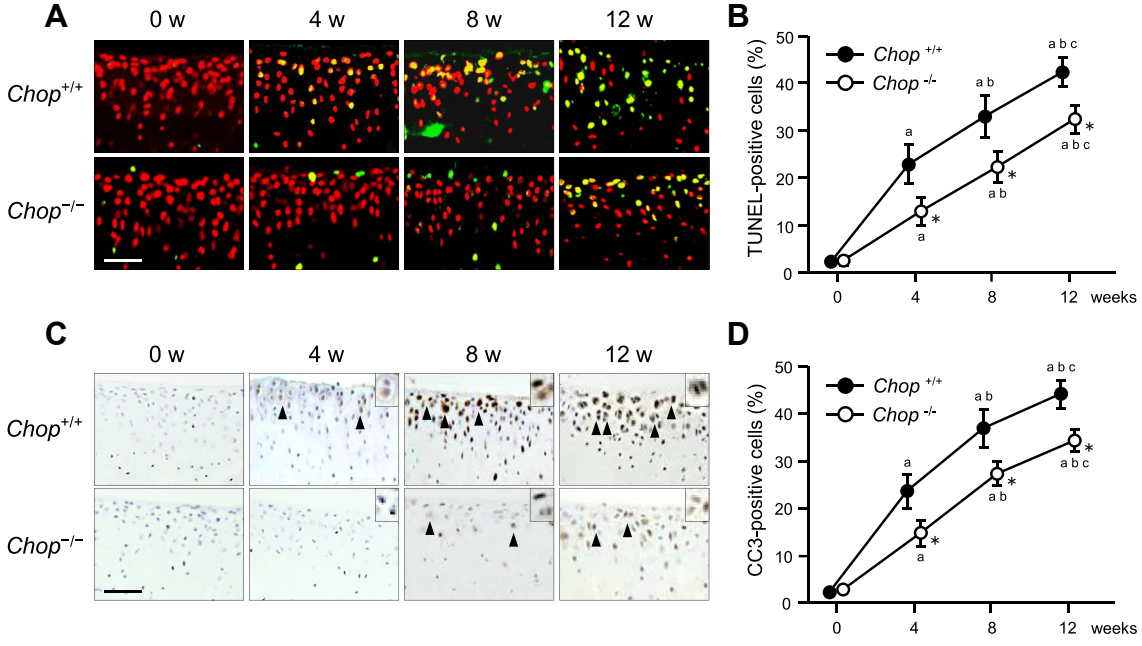

Fig. 2. Time course of TUNEL- and CC3-positive cells in a murine model of OA. The degree of DNA fragmentation and the CC3 expression were evaluated by TUNEL staining and CC3 immunostaining, and were analyzed semiquantitatively by the ratio of TUNEL- and CC3-positive cells ($n = 10$ per experimental group and time point). (A) TUNEL-positive cells in cartilage appeared gradually during the 12-week observation period in *Chop*$^{+/+}$- and *Chop*$^{-/-}$ mice. Their number was lower in *Chop*$^{-/-}$ mice. (B) The percentage of TUNEL-positive cells was significantly lower in *Chop*$^{-/-}$ mice at weeks 4, 8, and 12. (C) In *Chop*$^{+/+}$- and *Chop*$^{-/-}$ mice the number of CC3-positive cells increased gradually during the 12-week observation period. Their number was significantly lower in *Chop*$^{-/-}$ mice at weeks 4, 8, and 12. (D) The percentage of CC3-positive cells was significantly lower in *Chop*$^{-/-}$ mice at weeks 4, 8, and 12. Data are expressed as the mean (symbols) ± 95% confidence intervals (error bar). Scale bar = 50 μm, original magnification ×200. Arrows indicate positive cells. a = $P < 0.001$ vs week 0, b = $P < 0.001$ vs week 4, c = $P < 0.001$ vs week 8 in each group of mice by ANOVA with Bonferroni post hoc correction. *$P < 0.001$ vs *Chop*$^{+/+}$ mice by the Student's *t*-test.

Results

Murine OA model

In operated *Chop*$^{+/+}$- and *Chop*$^{-/-}$ mice, Safranin-O staining showed matrix degradation in the proximal tibial and distal femoral cartilage [Fig. 1(A)]. The strength of staining decreased gradually from 0 to 12 weeks in *Chop*$^{+/+}$ mice; this phenomenon was milder in *Chop*$^{-/-}$ mice. In the tibia the modified Mankin score at weeks 0, 4, 8, and 12 was 0.4, 17.2, 24.9, and 35.9 in *Chop*$^{+/+}$- and 0.3, 9.2, 14.5, and 24.3 in *Chop*$^{-/-}$ mice [Fig. 1(B)]. In the femur the score was 0.3, 18.1, 25.0, and 32.5 in *Chop*$^{+/+}$- and 0.2, 8.4, 13.1, and 21.4 in *Chop*$^{-/-}$ mice [Fig. 1(C)]. These scores were significantly lower in *Chop*$^{-/-}$- than *Chop*$^{+/+}$ mice.

TUNEL staining for apoptotic cells showed that in *Chop*$^{+/+}$ mice their number increased gradually from 0 to 12 weeks [Fig. 2(A)]; the increase was milder in *Chop*$^{-/-}$ mice. The percentage of TUNEL-positive cells at weeks 0, 4, 8, and 12 was 1.1%, 23.1%, 36.5%, and 45.4% in *Chop*$^{+/+}$- and 1.3%, 13.1%, 26.5%, and 33.2% in *Chop*$^{-/-}$ mice. The difference between the groups was statistically significant at 4, 8, and 12 weeks [Fig. 2(B)]. The number of CC3-positive cells increased gradually from 0 to 12 weeks [Fig. 2(C)]; the increase was milder in *Chop*$^{-/-}$ mice. The percentage of CC3-positive cells at weeks 0, 4, 8, and 12 was 0.3%, 21.9%, 35.1%, and 45.8% in *Chop*$^{+/+}$- and 0.3%, 12.0%, 21.3%, and 33.1% in *Chop*$^{-/-}$ mice. The difference was statistically significant at 4, 8, and 12 weeks [Fig. 2(D)].

Immunohistochemistry showed that the number of Chop-positive cells in *Chop*$^{+/+}$ mice increased from 0 to 12 weeks; no Chop-positive cells were observed in *Chop*$^{-/-}$ mice. The percentage of Chop-positive cells at week 0, 4, 8, and 12 was 3.1%, 12.8%, 15.9%, and 27.9% in *Chop*$^{+/+}$ mice. The differences between the two groups were significant [Fig. 3(A) and (B)].

The number of Xbp1s-positive cells was significantly higher in both groups at weeks 4, 8 and 12 than at week 0 [Fig. 3(C)]. The percentage of these cells at weeks 0, 4, 8, and 12, was 16.3%, 38.8%, 33.2%, and 31.2% in *Chop*$^{+/+}$- and 14.3%, 35.0%, 34.9%, and 32.5% in *Chop*$^{-/-}$ mice. There was no significant difference between the two groups [Fig. 3(D)].

The number of Grp78-positive cells in both *Chop*$^{+/+}$- and *Chop*$^{-/-}$ mice was higher at weeks 4, 8, and 12 than at week 0 [Fig. 3(E)]. Their percentage at week 0, 4, 8, and 12 was 24.7%, 42.8%, 44.2%, and 41.0% in *Chop*$^{+/+}$- and 26.8%, 45.0%, 46.9%, and 43.1% in *Chop*$^{-/-}$ mice. The percentage of Grp78-positive cells at 4, 8, and 12 was significantly higher than at week 0; the difference between the two groups was not significant [Fig. 3(F)].

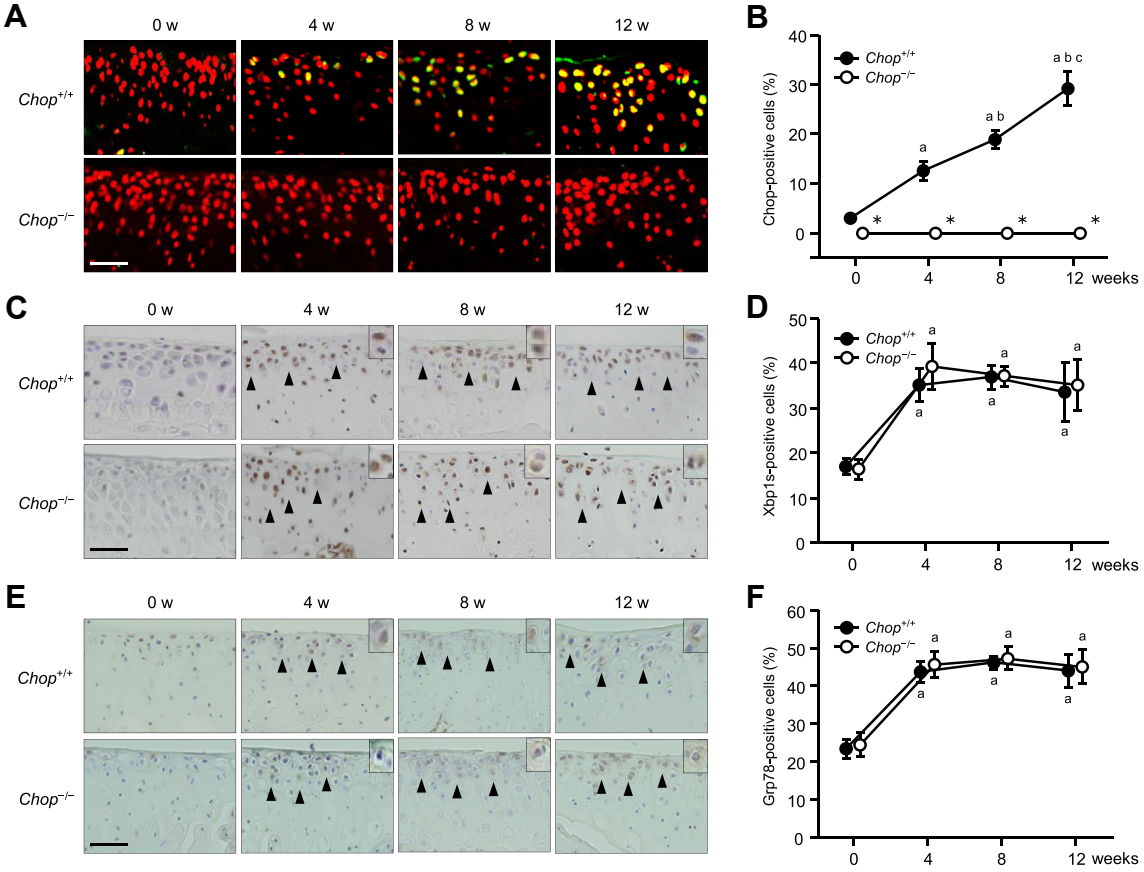

Fig. 3. Time course of ER stress in a murine model of OA. The expression levels of Chop, Xbp1s, and Grp78 in cartilage were evaluated immunohistochemically and analyzed semiquantitatively by calculating the total percentage of cells positive for each protein ($n = 10$ per experimental group and time point). (A) Chop-positive cells: In *Chop*$^{+/+}$ mice their number gradually increased from 0 to 12 weeks after surgery. *Chop*$^{-/-}$ mice were negative. (B) In *Chop*$^{+/+}$ mice, there was a significant difference in the percentage of Chop-positive cells at 0, 4, 8, and 12 weeks. There were significant differences between *Chop*$^{+/+}$- and *Chop*$^{-/-}$ mice at all time points. (C) Xbp1s-positive cells: In *Chop*$^{+/+}$- and *Chop*$^{-/-}$ mice their number was higher at 4, 8, and 12 weeks than at week 0. (D) In both groups, the percentage of these cells was significantly higher at 4, 8, and 12 weeks than at week 0. There was no significant difference between *Chop*$^{+/+}$- and *Chop*$^{-/-}$ mice. (E) Grp78-positive cells: In *Chop*$^{+/+}$- and *Chop*$^{-/-}$ mice, their number was higher at 4, 8, and 12 weeks than at week 0. (F) In both groups, the percentage of these cells was significantly higher at 4, 8, and 12 weeks than at week 0. There was no significant difference between *Chop*$^{+/+}$- and *Chop*$^{-/-}$ mice. Data are expressed as the mean (symbols) ± 95% confidence intervals (error bar). Scale bar = 50 μm, original magnification ×200. Arrows indicate positive cells. a = $P < 0.001$ vs week 0, b = $P < 0.001$ vs week 4, c = $P < 0.001$ vs week 8 in each group of mice by ANOVA with Bonferroni *post hoc* correction. *$P < 0.001$ vs *Chop*$^{+/+}$ mice by the Student *t*-test.

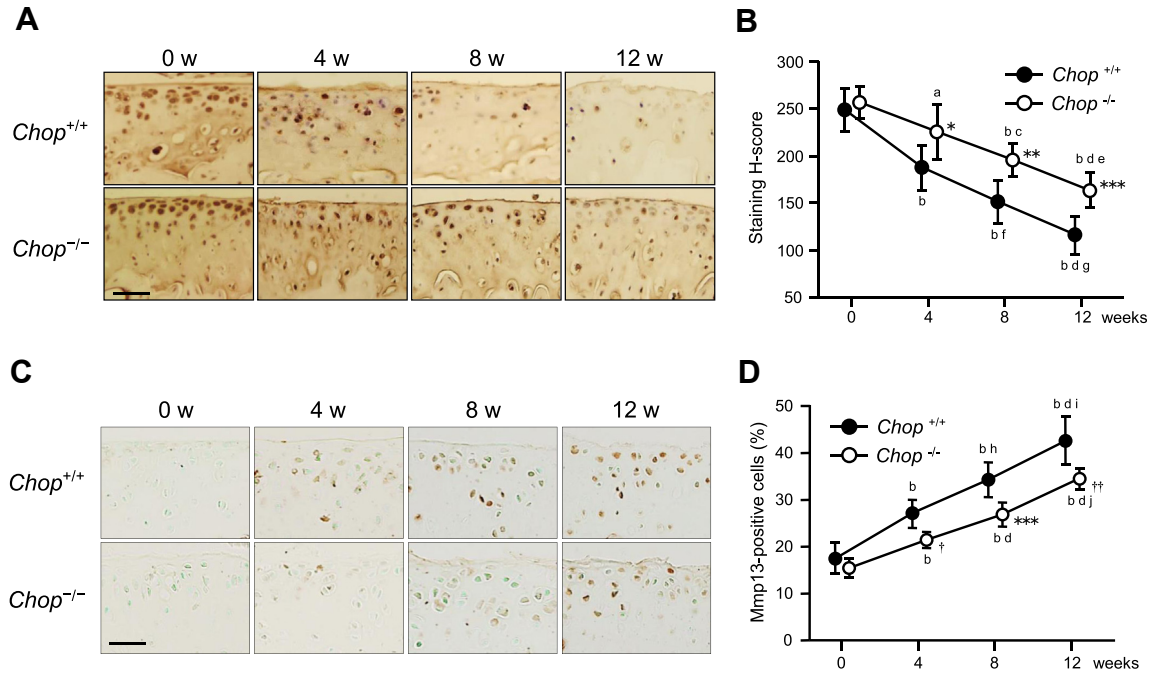

Fig. 4. Time course of chondrocyte metabolic function in a murine model of OA. The expression levels of Col2 and Mmp13 in cartilage were evaluated immunohistochemically. The Col2 expression was measured semiquantitatively with a staining H-score, and the Mmp13 expression was analyzed semiquantitatively by calculating the total percentage of cells positive ($n = 10$ per experimental group and time point). (A) Col2 expression: In both *Chop*$^{+/+}$- and *Chop*$^{-/-}$ mice, the strength of staining for Col2a gradually decreased during the 12-week observation period. This decrease was milder in *Chop*$^{-/-}$ mice. (B) In both *Chop*$^{+/+}$- and *Chop*$^{-/-}$ mice there was a significant difference in staining H-score at 0, 4, 8, and 12 weeks. There were significant differences between *Chop*$^{+/+}$- and *Chop*$^{-/-}$ mice at 4, 8, and 12 weeks. (C) Mmp13-positive cells: In *Chop*$^{+/+}$- and *Chop*$^{-/-}$ mice, their number increased gradually during the 12-week observation period; it was lower in *Chop*$^{-/-}$- than *Chop*$^{+/+}$ mice. (D) In both *Chop*$^{+/+}$- and *Chop*$^{-/-}$ mice there was a significant difference in the percentage of Mmp13-positive cells at 0, 4, 8, and 12 weeks. There were significant differences between *Chop*$^{+/+}$- and *Chop*$^{-/-}$ mice at 4, 8, and 12 weeks. Data are expressed as the mean (symbols) ± 95% confidence intervals (error bar). Scale bar = 50 μm, original magnification ×200. a = $P = 0.024$, b = $P < 0.001$ vs week 0; c = $P = 0.031$, d = $P < 0.001$, f = $P = 0.014$, h = $P = 0.005$ vs weeks 4; e = $P = 0.023$, g = $P = 0.017$, i = $P = 0.002$, j = $P < 0.001$ vs 8 weeks, respectively, by ANOVA with Bonferroni *post hoc* correction. $^{*}P = 0.037$, $^{**}P = 0.003$, $^{***}P = 0.001$, $^{\dagger}P = 0.002$, $^{\dagger\dagger}P = 0.005$ vs *Chop*$^{+/+}$ mice by the Student *t*-test.

The anabolic and catabolic function of chondrocytes was analyzed by immunohistochemistry for Col2 and Mmp13, respectively. Staining strength for Col2 decreased gradually from 0 to 12 weeks in *Chop*$^{+/+}$ mice [Fig. 4(A)]; this change was milder in *Chop*$^{-/-}$ mice. The staining H-score at weeks 0, 4, 8, and 12 was 249.0, 187.6, 151.2, and 116.2 in *Chop*$^{+/+}$- and 256.5, 225.2, 195.2, and 163.6 in *Chop*$^{-/-}$ mice [Fig. 4(B)]. These scores were significantly lower in *Chop*$^{-/-}$- than *Chop*$^{+/+}$ mice [Fig. 4(B)].

The number of Mmp13-positive cells increased gradually from 0 to 12 weeks [Fig. 4(C)]; this increase was milder in *Chop*$^{-/-}$ mice. The percentage of Mmp13-positive cells at weeks 0, 4, 8, and 12 was 18.8%, 27.5%, 33.4%, and 41.3% in *Chop*$^{+/+}$- and 15.3%, 20.1%, 27.4%, and 33.4% in *Chop*$^{-/-}$ mice. The difference between the two groups was statistically significant at 4, 8, and 12 weeks [Fig. 4(D)].

Cultured chondrocytes

The expression of *Chop* mRNA was 20.5 times higher in TM-treated- than untreated *Chop*$^{+/+}$ chondrocytes [Fig. 5(A)]. Neither *Chop* mRNA nor Chop protein expression was found in *Chop*$^{-/-}$ chondrocytes [Fig. 5(A) and (B)], confirming *Chop* gene knockout. The expression of *Grp78* mRNA was 13.5 times higher in TM-treated *Chop*$^{+/+}$- and 12.6 times higher in TM-treated *Chop*$^{-/-}$ chondrocytes than in TM-untreated cells, indicating that TM produces similar levels of ER stress in *Chop*$^{-/-}$- and *Chop*$^{+/+}$ chondrocytes [Fig. 5(C)]. The protein expression of Grp78 was increased equally in *Chop*$^{+/+}$- and *Chop*$^{-/-}$ chondrocytes [Fig. 5(D)]. The expression of *Xbp1s* mRNA was similarly up-regulated in *Chop*$^{+/+}$- and *Chop*$^{-/-}$ chondrocytes [Fig. 5(E)].

The number of TUNEL-positive cells with TM treatment was increased in *Chop*$^{+/+}$- and *Chop*$^{-/-}$ chondrocytes compared to TM-untreated chondrocytes, but it was less in *Chop*$^{-/-}$- than *Chop*$^{+/+}$ chondrocytes [Fig. 6(A)]. There were more cleaved caspase-3-positive cells in TM-treated *Chop*$^{+/+}$- than *Chop*$^{-/-}$ chondrocytes [Fig. 6(B)]. ELISA showed that TM increased the level of apoptosis 4.4-fold in *Chop*$^{+/+}$- and 2.0-fold in *Chop*$^{-/-}$ cells, but it was lower than in *Chop*$^{-/-}$- than *Chop*$^{+/+}$ chondrocytes [Fig. 6(C)].

Chondrocyte anabolic function was evaluated by the expression of *Col2a1* and *Acan* mRNA. After TM treatment, *Col2a1* mRNA expression was reduced by 71.2% in *Chop*$^{+/+}$- and by 50.0% in *Chop*$^{-/-}$ chondrocytes compared to TM-untreated chondrocytes, and the expression was significantly higher in *Chop*$^{-/-}$- than *Chop*$^{+/+}$ chondrocytes [Fig. 7(A)]. TM reduced the expression of *Acan* mRNA by 60.4% in *Chop*$^{+/+}$- and by 37.1% in *Chop*$^{-/-}$ chondrocytes compared to TM-untreated chondrocytes, and the expression was significantly higher in *Chop*$^{-/-}$- than *Chop*$^{+/+}$ chondrocytes [Fig. 7(B)]. By TM treatment, the expression of *Mmp13* mRNA, analyzed as a chondrocyte catabolic function, was increased by 43.9% in *Chop*$^{+/+}$- and by 35.1% in *Chop*$^{-/-}$ chondrocytes compared to TM-untreated chondrocytes [Fig. 7(C)]. The expression was significantly lower in *Chop*$^{-/-}$- than *Chop*$^{+/+}$ chondrocytes with or without TM treatment [Fig. 7(C)].

Discussion

Using our mouse model of OA we investigated ER stress, apoptosis, and cartilage degeneration *in vivo* and *in vitro*. The expression of Chop and apoptosis increased significantly in *Chop*$^{+/+}$ mice as degeneration progressed. While ER stress was similar in

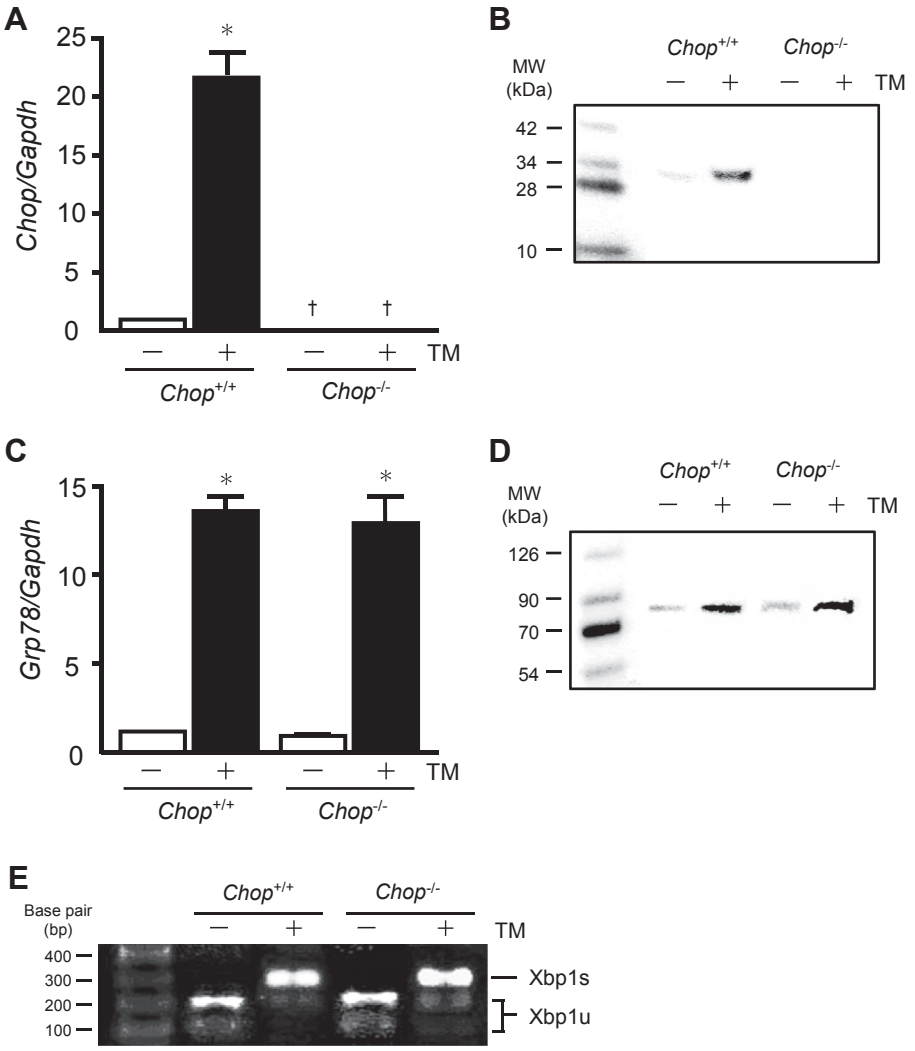

Fig. 5. Evaluation of ER stress in chondrocytes. ER stress in chondrocytes was evaluated by the expression of Chop, Grp78, and Xbp1s. Three independent experiments were performed, and the data was analyzed in triplicate. (A) The expression of *Chop* mRNA was increased by TM in *Chop*$^{+/+}$- and *Chop*$^{-/-}$ chondrocytes; the increase was significantly less in *Chop*$^{-/-}$- than *Chop*$^{+/+}$ cells. (B) The protein expression of Chop (MW 30 kDa) was increased by TM in *Chop*$^{+/+}$ chondrocytes, but was not confirmed in *Chop*$^{-/-}$ cells. (C) The expression of *Grp78* mRNA was increased by TM in both groups; the difference between them was not significant. (D) The protein expression of Grp78 (MW 78 kDa) was increased equally by TM in both groups. (E) The *Xbp1s* PCR products were subsequently visualized as 323 bp and *Xbp1u* PCR products were separated into 228- and 116 bp. The expression of *Xbp1s* mRNA was increased in both groups by TM. Data are expressed as the mean (symbols) ± 95% confidence intervals (error bar). *$P < 0.001$ vs TM^{-}, †$P < 0.001$ vs *Chop*$^{+/+}$ (Student's *t*-test).

Chop$^{-/-}$- and *Chop*$^{+/+}$ mice, apoptosis and the degree of degeneration were significantly lower in *Chop*$^{-/-}$ mice. ER stress was mediated equally by TM in cultured chondrocytes; however, the increase in apoptosis and the decrease in *Col2a1* and *Acan* mRNA expression in *Chop*$^{-/-}$ cells were significantly less than *Chop*$^{+/+}$ cells.

The expression of Chop, an apoptosis-related molecule, and the degree of apoptosis were increased in cultured chondrocytes treated with ER stress inducers[15,16,27] and related to the progression of cartilage degeneration in human OA cartilage[15], suggesting the involvement of Chop-mediated, ER stress-induced apoptosis. We document that increased Chop expression and apoptosis were also related with progressive cartilage degeneration in mice.

Elsewhere[19] we reported that the degree of cartilage degeneration in *Chop*$^{-/-}$ mice was significantly less than *Chop*$^{+/+}$ mice; but we did not address chondrocyte apoptosis and assessments were performed 4 weeks after surgery. In the present study we focused on the role of Chop in cartilage degeneration from the perspectives of ER stress induction and apoptosis. We present a comprehensive evaluation of apoptosis *via* ER stress pathways and of cartilage degeneration by analyzing the 12-week time course of cartilage degeneration, apoptosis, and the ER stress markers Xbp1s, Grp78, and Chop.

The status of our OA model at 8 and 12 weeks after surgery corresponds to human early and moderate OA, respectively[21,28,29]. We found that chondrocyte apoptosis contributed to cartilage degeneration, changes that were less marked by the suppression of *Chop* gene expression. Chop leads to a decrease in anti-apoptotic Bcl-2 protein, activates pro-apoptotic factors such as Bim and Bax, and induces apoptosis through the activation of caspases[13,30,31]. In murine cortical neurons[32] and human carcinoma cells[33], Chop-mediated caspase-3 activation induces apoptosis. The increase in CC3 with cartilage degeneration was less in *Chop*$^{-/-}$- than *Chop*$^{+/+}$ mice, suggesting that Chop also induces apoptosis in chondrocytes *via* caspase activation.

In TM-treated cultured *Chop*$^{+/+}$ chondrocytes, chondrocyte apoptosis was significantly increased; *Col2a* and *Acan* mRNA expression was significantly down-regulated and *Mmp13* mRNA

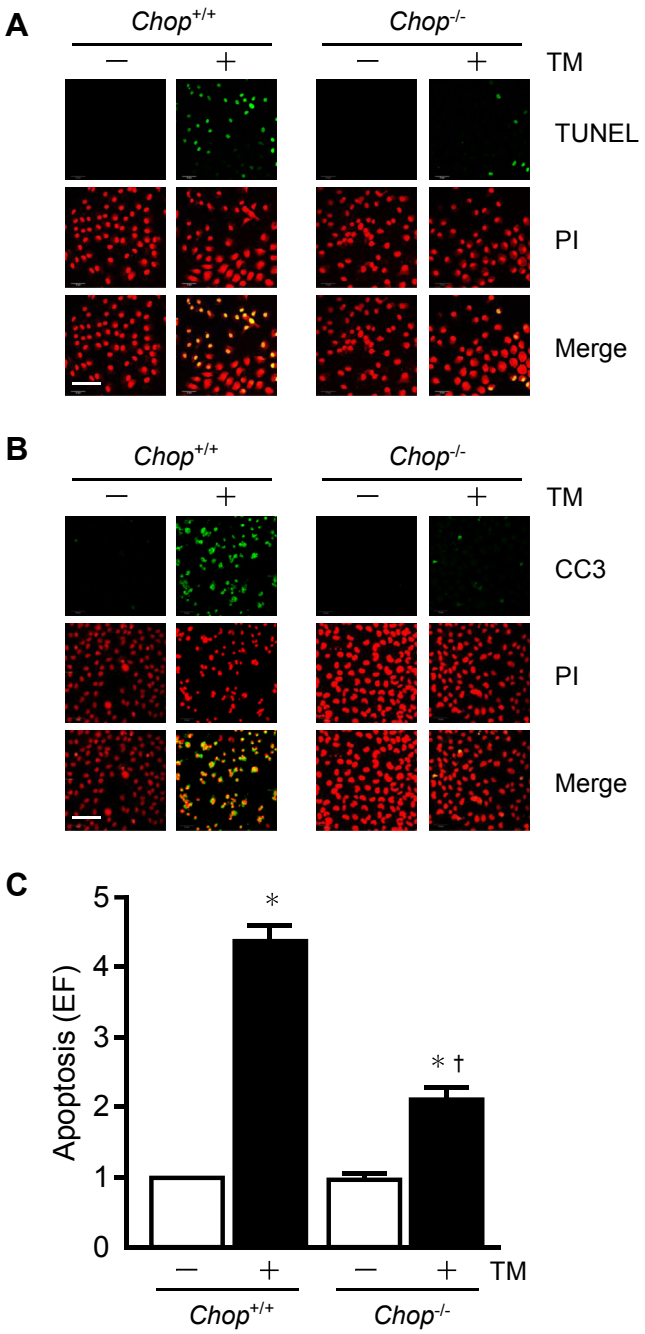

Fig. 6. Evaluation of apoptosis in cultured chondrocytes. The degree of apoptosis in cultured chondrocytes was evaluated by DNA fragmentation and CC3 expression. Three independent experiments were performed, and the data was analyzed in triplicate. (A) TUNEL staining: TUNEL-positive cells were increased by TM in *Chop*$^{+/+}$- and *Chop*$^{-/-}$ chondrocytes. The increase was less in *Chop*$^{-/-}$- than *Chop*$^{+/+}$ cells. (B) CC3 immunostaining: CC3-positive cells were increased by TM in *Chop*$^{+/+}$- and *Chop*$^{-/-}$ chondrocytes; the increase was less in *Chop*$^{-/-}$- than *Chop*$^{+/+}$ cells. (C) ELISA showed that the level of apoptosis was increased by TM in both groups. This increase was less in *Chop*$^{-/-}$- than *Chop*$^{+/+}$ cells. Scale bar = 100 μm, original magnification ×200. Data are expressed as the mean (symbols) ± 95% confidence intervals (error bar). *$P < 0.001$ vs TM^{-}, †$P < 0.001$ vs *Chop*$^{+/+}$ (Student's *t*-test).

expression was significantly up-regulated. These changes were less marked in *Chop*$^{-/-}$ chondrocytes. In *Chop*$^{+/+}$ mice, chondrocyte apoptosis was significantly increased, the expression of Col2 and Acan, containing numerous glycosaminoglycan chains stained by Safranin-O[34,35] was decreased, and Mmp13 expression was significantly increased with progressive cartilage degeneration; these changes were suppressed in *Chop*$^{-/-}$ mice. Others[7,36,37] reported that suppressed ECM gene expression mediated by mechanical stress recovered upon inhibition of chondrocyte apoptosis. We obtained genetic evidence that Chop plays a direct role in chondrocyte metabolism under conditions of increased ER stress and influences the rate of apoptosis, and that Chop ablation reduced the severity of OA in our model.

Our *in vivo* and *in vitro* studies showed no difference with respect to the manifestation of ER stress regardless of *Chop* gene deletion. When unfolded proteins are accumulated in the ER, the activation of Ire1α results in the splicing of Xbp1s which then induces genes encoding for the ER chaperone protein and ER-associated degradation[8,38,39]. Grp78, an ER chaperone, promotes protein folding[40]. Although UPRs help to maintain cellular homeostasis, excessive ER stress mediates Chop expression and leads to a switch from protective to pro-apoptotic signaling[31]. As Grp78 and Xbp1s expression in *Chop*$^{-/-}$ mice and *Chop*$^{-/-}$ chondrocytes was similar to that seen in cells from *Chop*$^{+/+}$ mice, we suggest that there was no difference in the manifestation of ER stress and that the function to maintain homeostasis did not depend on the *Chop* gene.

In human OA cartilage, CHOP expression increased with degeneration and the expression of XBP1s was up-regulated in moderate- but down-regulated in severe OA[15], indicating that in severe OA, apoptotic signaling superseded the maintenance of homeostasis. The expression of Grp78, Xbp1s, and Chop in *Chop*$^{+/+}$ mice was higher at week 4 than week 0 and while there was no significant difference in the expression of Grp78 and Xbp1s at 4- and 8 weeks, Chop expression was increased at 8 weeks. This points to a switching in UPR signaling between weeks 4 and 8, and is consistent with a higher degree of apoptosis at 8 weeks. *In vitro*, the increase in apoptosis and the decrease in chondrocyte function were suppressed in *Chop*$^{-/-}$ chondrocytes, suggesting that the acceleration of apoptosis by increased Chop expression plays a role in the progression of cartilage degeneration.

In the earlier phases of OA cartilage degeneration, the progressive cartilage destruction preceded chondrocyte apoptosis[41]. In our study apoptosis started to emerge at week 4 and we assessed ER stress-induced apoptosis *via* Chop in cartilage degeneration. A significant difference in early pre-apoptosis OA between *Chop*$^{+/+}$- and *Chop*$^{-/-}$ mice with respect to aggrecan or collagen loss would suggest that Chop affects cartilage degeneration *via* a pathway that is unrelated to apoptosis. There is currently no evidence that Chop directly regulates cartilage metabolism. According to Hayashida *et al.*[42], in humans C/EBP β directly bound to the *Mmp13* promoter region. Like Chop, C/EBP β belongs to the C/EBP family, and their function is inhibited by the dominant-negative effect of Chop[43]. The *Mmp13* mRNA expression was down-regulated in our TM-untreated *Chop*$^{-/-}$ chondrocytes, suggesting Chop involvement in the expression of Mmp13. Studies using *Chop*$^{-/-}$ mice are underway to determine the influence of the non-apoptotic function of Chop on cartilage degeneration.

Our study has some limitations. In humans, OA is a gradually progressing degenerative disease. As we surgically produced joint instability in mice, their disease progression was hastened. However, the pathologic features of this widely-used OA model[29,44,45] are similar to those in human OA[21]. We cannot rule out the existence of ER stress-induced pathways other than Chop. *In vivo*, we did not show direct evidence that ER stress caused chondrocyte apoptosis. *In vitro*, ER stress-induced apoptosis was not completely suppressed in *Chop*$^{-/-}$ chondrocytes. The ER stress-induced apoptosis was also induced by c-Jun N-terminal kinases other than Chop[31]. It was previously reported that apoptosis had been induced by the crosstalk of ER stress and oxidative stress[46]. We

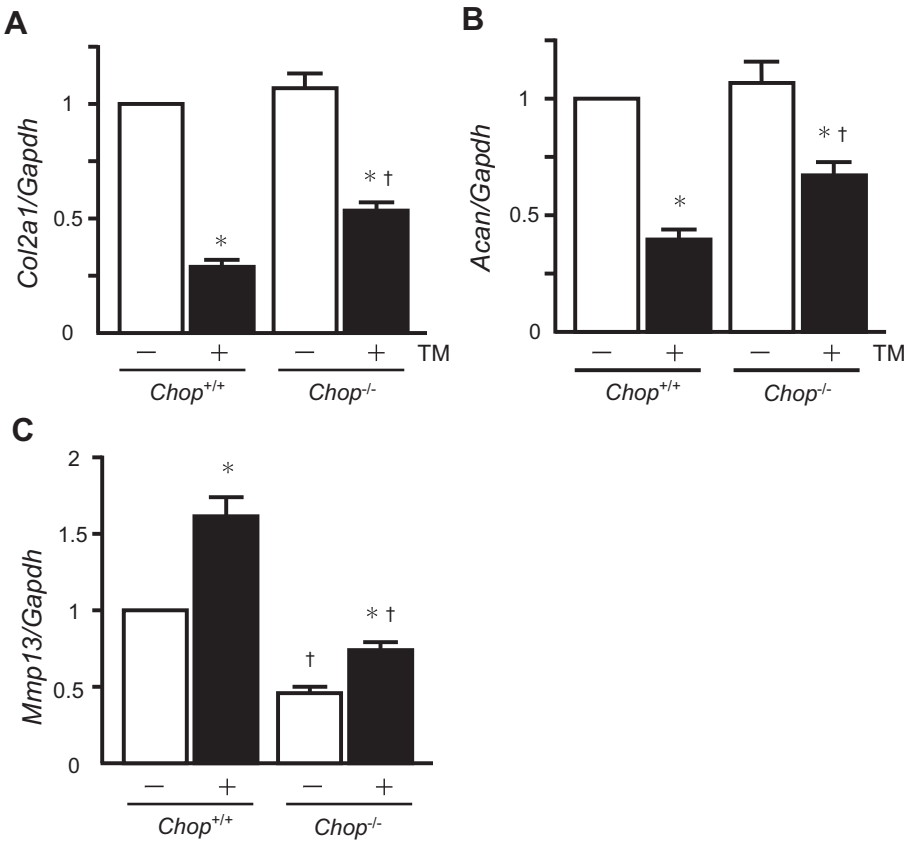

Fig. 7. Evaluation of chondrocyte function in cultured chondrocytes. The chondrocyte function in cultured chondrocytes was evaluated by *Col2a1*, *Acan*, and *Mmp13* mRNA expression. Three independent experiments were performed, and the data was analyzed in triplicate. (A) The expression of *Col2a1* mRNA was decreased by TM in $Chop^{+/+}$- and $Chop^{-/-}$ chondrocytes. The expression in $Chop^{-/-}$ cells was significantly higher than in $Chop^{+/+}$ cells. (B) The expression of *Acan* mRNA in both groups was suppressed by TM. Its expression was significantly higher in $Chop^{-/-}$- than $Chop^{+/+}$ cells. (C) The expression of *Mmp13* mRNA was increased by TM in both $Chop^{+/+}$- and $Chop^{-/-}$ chondrocytes. Its expression was significantly lower in $Chop^{-/-}$- than $Chop^{+/+}$ cells with or without TM. Data are expressed as the mean (symbols) ± 95% confidence intervals (error bar). $^{*}P < 0.001$ vs TM^{-}, $^{\dagger}P < 0.001$ vs $Chop^{+/+}$ (Student's *t*-test).

need to investigate the relationship between these mediators and ER stress in our OA model.

$Chop^{-/-}$ mice have been used in various disease models that investigated the role of apoptosis in disease progression[11,14,47]. Our surgical model of OA in mice shows that chondrocyte apoptosis *via* Chop induction contributes to the progression of cartilage degeneration and that Chop plays an important role in the pathology of OA. Our findings suggest that Chop may become a molecular therapeutic target for OA.

Contributions

All authors made substantial contributions to all three sections: (1) the conception and design of the study, or acquisition of data or analysis and interpretation of data, (2) drafting the article and revising it critically for important intellectual content, (3) final approval of the version to be submitted. J Hirose (hirojun-mk@umin.ac.jp) took responsibility for the integrity of the work as a whole, from inception to completion.

Role of the funding source

This work was supported in part by a Grant-in-Aid for Scientific Research from the Japanese Ministry of Education, Culture, Sports, Science, and Technology (11009506).

Conflict of interests

The authors have no conflicts of interest to declare.

Acknowledgments

We thank Dr Yuichi Oike for providing the $Chop^{-/-}$ mice. We also thank Drs Tomomi Gotoh, Kei Senba, and Koji Takada for their excellent technical assistance.

References

1. Wei L, Sun XJ, Wang Z, Chen Q. CD95-induced osteoarthritic chondrocyte apoptosis and necrosis: dependency on p38 mitogen-activated protein kinase. Arthritis Res Ther 2006;8:R37.
2. Thomas CM, Fuller CJ, Whittles CE, Sharif M. Chondrocyte death by apoptosis is associated with cartilage matrix degradation. Osteoarthritis Cartilage 2007;15:27–34.
3. Heraud F, Heraud A, Harmand MF. Apoptosis in normal and osteoarthritic human articular cartilage. Ann Rheum Dis 2000;59:959–65.
4. Sharif M, Whitehouse A, Sharman P, Perry M, Adams M. Increased apoptosis in human osteoarthritic cartilage corresponds to reduced cell density and expression of caspase-3. Arthritis Rheum 2004;50:507–15.
5. Blanco FJ, Guitian R, Vázquez-Martul E, de Toro FJ, Galdo F. Osteoarthritis chondrocytes die by apoptosis: a possible pathway for osteoarthritis pathology. Arthritis Rheum 1998;41:284–9.

6. Hashimoto S, Ochs RL, Komiya S, Lotz M. Linkage of chondrocyte apoptosis and cartilage degradation in human osteoarthritis. Arthritis Rheum 1998;41:1632–8.
7. Kühn K. Cell death in cartilage. Osteoarthritis Cartilage 2004;12:1–16.
8. Ron D, Walter P. Signal integration in the endoplasmic reticulum unfolded protein response. Nat Rev Mol Cell Biol 2007;8:519–29.
9. Gotoh T, Endo M, Oike Y. Endoplasmic reticulum stress-related inflammation and cardiovascular diseases. Int J Inflam 2011;2011:259462.
10. Morishima N, Nakanishi K, Takenouchi H, Shibata T, Yasuhiko Y. An endoplasmic reticulum stress-specific caspase cascade in apoptosis. Cytochrome c-independent activation of caspase-9 by caspase-12. J Biol Chem 2002;277:34287–94.
11. Oyadomari S, Koizumi A, Takeda K, Gotoh T, Akira S, Araki E, *et al*. Targeted disruption of the Chop gene delays endoplasmic reticulum stress-mediated diabetes. J Clin Invest 2002;109:525–32.
12. Puthalakath H, O'Reilly LA, Gunn P, Lee L, Kelly PN, Huntington ND, *et al*. ER stress triggers apoptosis by activating BH3-only protein Bim. Cell 2007;129:1337–49.
13. Oyadomari S, Mori M. Roles of CHOP//GADD153 in endoplasmic reticulum stress. Cell Death Differ 2003;11:381–9.
14. Fu HY, Okada K, Liao Y, Tsukamoto O, Isomura T, Asai M, *et al*. Ablation of C/EBP homologous protein attenuates endoplasmic reticulum-mediated apoptosis and cardiac dysfunction induced by pressure overload. Circulation 2010;122:361–9.
15. Takada K, Hirose J, Senba K, Yamabe S, Oike Y, Gotoh T, *et al*. Enhanced apoptotic and reduced protective response in chondrocytes following endoplasmic reticulum stress in osteoarthritic cartilage. Int J Exp Pathol 2011;92:232–42.
16. Nugent AE, McBurney DL, Horton Jr WE. The presence of extracellular matrix alters the chondrocyte response to endoplasmic reticulum stress. J Cell Biochem 2011;112:1118–29.
17. Hamamura K, Goldring MB, Yokota H. Involvement of p38 MAPK in regulation of MMP13 mRNA in chondrocytes in response to surviving stress to endoplasmic reticulum. Arch Oral Biol 2009;54:279–86.
18. Takada K, Hirose J, Yamabe S, Uehara Y, Mizuta H. Endoplasmic reticulum stress mediates nitric oxide-induced chondrocyte apoptosis. Biomed Rep 2013;1:315–9.
19. Yamabe S, Hirose J, Uehara Y, Okada T, Okamoto N, Oka K, *et al*. Intracellular accumulation of advanced glycation end products induces apoptosis via endoplasmic reticulum stress in chondrocytes. FEBS J 2013;280:1617–29.
20. Oyadomari S, Takeda K, Takiguchi M, Gotoh T, Matsumoto M, Wada I, *et al*. Nitric oxide-induced apoptosis in pancreatic beta cells is mediated by the endoplasmic reticulum stress pathway. Proc Natl Acad Sci (USA) 2001;98:10845–50.
21. Kamekura S, Hoshi K, Shimoaka T, Chung U, Chikuda H, Yamada T, *et al*. Osteoarthritis development in novel experimental mouse models induced by knee joint instability. Osteoarthritis Cartilage 2005;13:632–41.
22. Kozawa E, Nishida Y, Cheng XW, Urakawa H, Arai E, Futamura N, *et al*. Osteoarthritic change is delayed in a *Ctsk*-knockout mouse model of osteoarthritis. Arthritis Rheum 2012;64:454–64.
23. Moldovan F, Pelletier J-P, Hambor J, Cloutier J-M, Martel-Pelletier J. Collagenase-3 (matrix metalloprotease 13) is preferentiall y localized in the deep layer of human arthritic cartilage *in situ. In vitro* mimicking effect by transforming growth factor β. Arthritis Rheum 1997;40:1653–61.
24. Wimsey S, Lien CF, Sharma S, Brennan PA, Roach HI, Harper GD, *et al*. Changes in immunolocalisation of β-dystroglycan and specific degradative enzymes in the osteoarthritic synovium. Osteoarthritis Cartilage 2006;14:1181–8.
25. Uehara T, Nakamura T, Yao D, Shi Z-Q, Gu Z, Ma Y, *et al*. S-Nitrosylated protein-disulphide isomerase links protein misfolding to neurodegeneration. Nature 2006;441:513–7.
26. Lowry OH, Rosebrough NJ, Farr AL, Randall RJ. Protein measurement with the Folin phenol reagent. J Biol Chem 1951;193:265–75.
27. Oliver BL, Cronin CG, Zhang-Benoit Y, Goldring MB, Tanzer ML. Divergent stress responses to IL-1beta, nitric oxide, and tunicamycin by chondrocytes. J Cell Physiol 2005;204:45–50.
28. Glasson SS, Blanchet TJ, Morris EA. The surgical destabilization of the medial meniscus (DMM) model of osteoarthritis in the 129/SvEv mouse. Osteoarthritis Cartilage 2007;15:1061–9.
29. Kamekura S, Kawasaki Y, Hoshi K, Shimoaka T, Chikuda H, Maruyama Z, *et al*. Contribution of runt-related transcription factor 2 to the pathogenesis of osteoarthritis in mice after induction of knee joint instability. Arthritis Rheum 2006;54:2462–70.
30. Nakayama Y, Endo M, Tsukano H, Mori M, Oike Y, Gotoh T. Molecular mechanisms of the LPS-induced non-apoptotic ER stress-CHOP pathway. J Biochem 2010;147:471–83.
31. Szegezdi E, Logue SE, Gorman AM, Samali A. Mediators of endoplasmic reticulum stress-induced apoptosis. EMBO Rep 2006;7:880–5.
32. Galehdar Z, Swan P, Fuerth B, Callaghan SM, Park DS, Cregan SP. Neuronal apoptosis induced by endoplasmic reticulum stress is regulated by ATF4-CHOP-mediated induction of the Bcl-2 homology 3-only member PUMA. J Neurosci 2010;30:16938–48.
33. Yamaguchi H, Wang HG. CHOP is involved in endoplasmic reticulum stress-induced apoptosis by enhancing DR5 expression in human carcinoma cells. J Biol Chem 2004;279:45495–502.
34. Mackay AM, Beck SC, Murphy JM, Barry FP, Chichester CO, Pittenger MF. Chondrogenic differentiation of cultured human mesenchymal stem cells from marrow. Tissue Eng 1998;4:415–28.
35. Trowbridge JM, Gallo RL. Dermatan sulfate: new functions from an old glycosaminoglycan. Glycobiology 2002;12:117R–25R.
36. D'Lima DD, Hashimoto S, Chen PC, Lotz MK, Colwell Jr CW. Prevention of chondrocyte apoptosis. J Bone Joint Surg 2001;83:S25–6.
37. D'Lima D, Hermida J, Hashimoto S, Colwell C, Lotz M. Caspase inhibitors reduce severity of cartilage lesions in experimental osteoarthritis. Arthritis Rheum 2006;54:1814–21.
38. Ozcan U, Cao Q, Yilmaz E, Lee A-H, Iwakoshi NN, Ozdelen E, *et al*. Endoplasmic reticulum stress links obesity, insulin action, and type 2 diabetes. Science 2004;306:457–61.
39. Okada K, Minamino T, Tsukamoto Y, Liao Y, Tsukamoto O, Takashima S, *et al*. Prolonged endoplasmic reticulum stress in hypertrophic and failing heart after aortic constriction: possible contribution of endoplasmic reticulum stress to cardiac myocyte apoptosis. Circulation 2004;110:705–12.
40. Ni M, Lee AS. ER chaperones in mammalian development and human diseases. FEBS Lett 2007;581:3641–51.
41. Aigner T, McKenna L. Molecular pathology and pathobiology of osteoarthritic cartilage. Cell Mol Life Sci 2002;59:5–18.
42. Hayashida M, Okazaki K, Fukushi J, Sakamoto A, Iwamoto Y. CCAAT/enhancer binding protein beta mediates expression of matrix metalloproteinase 13 in human articular chondrocytes in inflammatory arthritis. Arthritis Rheum 2009;60:708–16.

43. Ron D, Habener JF. CHOP, a novel developmentally regulated nuclear protein that dimerizes with transcription factors C/EBP and LAP and functions as a dominant-negative inhibitor of gene transcription. Genes Dev 1992;6:439–53.
44. Shimizu S, Asou Y, Itoh S, Chung UI, Kawaguchi H, Shinomiya K, *et al*. Prevention of cartilage destruction with intraarticular osteoclastogenesis inhibitory factor/osteoprotegerin in a murine model of osteoarthritis. Arthritis Rheum 2007;56:3358–65.
45. Yamakawa K, Kamekura S, Kawamura N, Saegusa M, Kamei D, Murakami M, *et al*. Association of microsomal prostaglandin E synthase 1 deficiency with impaired fracture healing, but not with bone loss or osteoarthritis, in mouse models of skeletal disorders. Arthritis Rheum 2008;58:172–83.
46. Harding HP, Zhang Y, Zeng H, Novoa I, Lu PD, Calfon M, *et al*. An integrated stress response regulates amino acid metabolism and resistance to oxidative stress. Mol Cell 2003;11:619–33.
47. Namba T, Tanaka K-I, Ito Y, Ishihara T, Hoshino T, Gotoh T, *et al*. Positive role of CCAAT/enhancer-binding protein homologous protein, a transcription factor involved in the endoplasmic reticulum stress response in the development of colitis. Am J Pathol 2009;174:1786–98.